Proceedings of the Tenth (2013) ISOPE Ocean Mining and Gas Hydrates Symposium **www.isope.org**
Szczecin, Poland, September 22-26, 2013

ISBN 978-1-880653-92-0; ISSN 1946-0066

Axial Symmetrical Thermal Conduction and Phase Transformations in THF Hydrate-Bearing Sediments

Xu Hui Zhang Xiao Bing Lu

Key Laboratory of Fluid-Solid Coupling System Mechanics, Institute of mechanics, Chinese Academy of Sciences, Beijing, China

Shi Yao Hong Xia Zhen

Marine Environmental and Engineering Geological Survey, Guangzhou Marine Geological Survey Guangzhou, China

ABSTRACT

Thermal conduction and phase transformation are physical-chemical processes during the dissociation of gas hydrate-bearing sediments. Heat transfer leads to the expansion of hydrate dissociation front and the weakening of soils accompanied by the seepage of fluids and the deformation of sediments. As a consequence, ground failure may occur which can damage engineering structures and lead to environmental disasters. Hydrate dissociation in sediments is investigated using tetrahydrofuran (THF) hydrate sediments under various thermal strengths, and the time-dependent development of a hydrate-dissociation front is elucidated. An axial-symmetrical theoretical model and a numerical method are proposed based on experimental observations and analysis of the physical processes. Numerical and experimental results for evolution of the hydrate-dissociation front are in good agreement.

KEY WORDS: Hydrate; dissociation; phase transformation front; thermal conduction; axial symmetry.

INTRODUCTION

Natural gas hydrate is a crystalline solid composed mainly of methane gas and water molecules, and is stabilized under high-P/low-T conditions. Vast quantities of methane are trapped in ocean, continental margin and deep lake sediments in the form of hydrate and extraction of methane from hydrates could provide an important future energy resource (Kvenvolden and Lorenson, 2001; Hisashi, et al., 2002; Riedel, et al., 2006).

Hydrate-bearing sediments (HBS) may destabilize during exploitation or exploration. Both processes will directly change the strength of the hydrate-bearing sediments (Briaud and Chaouch, 1997; Zhang, et al, 2012). If the released gas is not released quickly, excess pore gas pressure will form and reduce the strength of the hydrate-bearing sediments. This may lead to environmental disasters, damage or destruction of ocean drilling platforms and oil wells, or even gas blowouts (Sultan, et al., 2004; Xu & Germanovich, 2006; Kwon, et al., 2008; Waite, et al., 2008).

Gas hydrate exploitation from ocean sediments (Fig. 1a) and oil or gas exploration is now extending for considerable distances from the continental shelf where hydrates may be present in relatively shallow layers below the seabed (Fig. 1b). There is a concern that hydrocarbon exploration and developmental activities may trigger hydrate dissociation and the axial symmetrical expansion of a hydrate dissociation zone which may lead to in seabed instability and damage of the local drilling well or well foundation (Chaouch and Briaud, 1997). The recent Deepwater Horizon explosion in the Gulf of Mexico might have been caused by the dissociation of methane hydrate since drilling had penetrated sediments where P-T conditions were appropriate for hydrate formation (Brooks, et al., 1986; Zhang, et al., 2011).

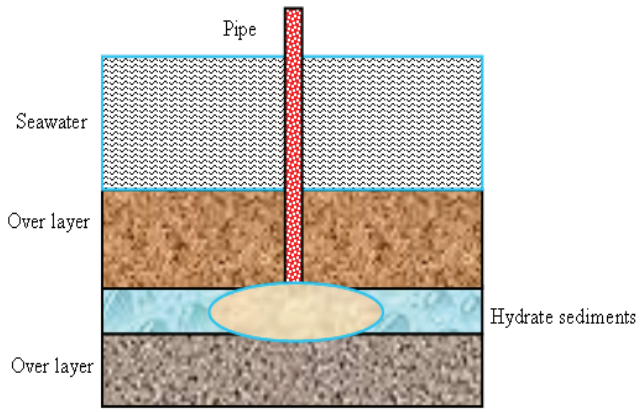

(a) hydrate exploitation

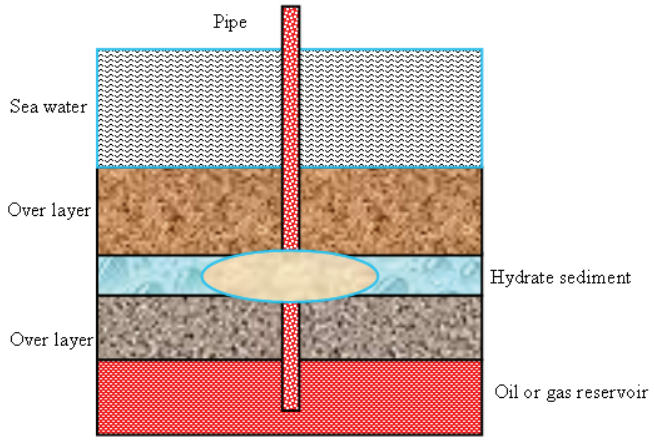

(b) oil or gas exploration

Fig. 1. Engineering background conditions for hydrate exploitation compared with that of oil or gas exploitation

The expansion of the hydrate dissociation zone induced by an oil pipe with a temperature of 100℃ in hydrate-bearing sediments was studied based on heat conduction theory (Briaud and Chaouch, 1997). The hydrate dissociation front around the oil pipe with a diameter of 1m was found to reach 20m after 15 years, and 30m after 40 years. The dissociation of gas hydrate in this zone can cause damage to the pipe.

Several analytical and numerical studies on expansion of the hydrate dissociation zone in hydrate-bearing sediments have been processed by combining the kinetic hydrate dissociation, gas and water seepage, heat conduction and energy conservation (Kimoto, et al., 2010; Klar, et al., 2010). However, analytical solutions are difficult to obtain and the numerical simulation needs to be verified by experimental results or in-situ data.

Bulk THF hydrate-bearing sediment can be synthesized more uniform, easily, safely and economically than methane hydrate sediment (MH), since THF can be completely miscible with water in any concentration and can form hydrate at the atmosphere pressure and a temperature < 4 ℃ (Tohidi, et al., 2001; Jones, et al., 2007). The physical and thermal properties of THF hydrate are similar to those of MH. Hence THF sediments are often used as a substitute for methane hydrate in experiments, especially for thermal simulation (Yun et al., 2007; Lee et al., 2007; Zhang, et al., 2010).

The aim of this paper is to study the heat-induced axial symmetrical evolution of the hydrate dissociation zone and the phase transformations during dissociation of the hydrate-bearing sediments. First, an axi-symmetrical apparatus was constructed and a series of experiments using THF hydrate sediments were carried out. Second, an axial-symmetrical model was presented considering the three-phase transformation fronts in sediments. Finally, the theoretical and numerical results were compared under the same geometries.

EXPERIMENTAL TECHNIQUES

The experimental set-up is as follows: thermal dissociation experiments using THF hydrate sediments with a size of diameter × height = 28 cm × 30 cm were conducted in an organic glass cylinder, simulating the heating induced axi-symmetrical evolution of hydrate dissociation and phase transformations. An immersion heater of 400 W, with a radius of 4 cm and a height of 12 cm, was positioned vertically at the axial centre to provide heat sources of different temperature, and a 2 cm-thick ceramic plate was placed at the bottom of the cylinder as a heat insulator. A liquid or gas inlet was inserted at the base of the cylinder to saturate the sediments with THF and water solution. Temperature sensors were arranged horizontally at 2 cm intervals within the middle of the sediment column, recording the evolution of the temperature and the dissociation front. A camera and an infrared thermometer were used to record the expansion of the transformation fronts at the upper surface of the sediments in real time (Fig. 2).

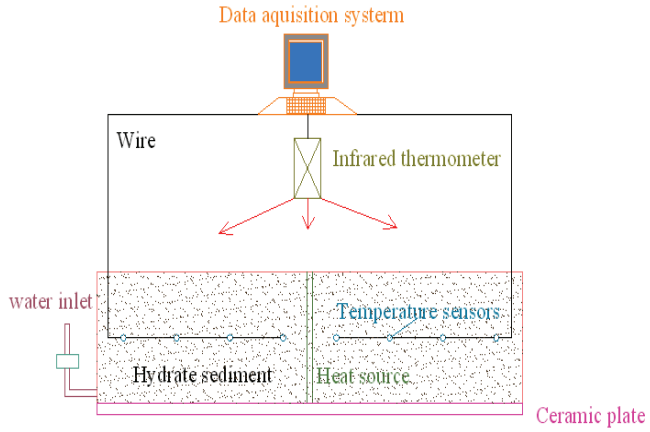

Fig. 2. The experimental set-up

Experimental procedures were as follows:

(1) A heat source with a temperature regulator and several temperature sensors were placed at the designated locations and the silty-sand sediment sample with a density of 1.6g/cm3 was compacted to a height of 15 cm from the base of the cylinder.

(2) The sand sample was saturated with THF liquor with a mass fraction of 19% through the inlet. The cylinder was then placed in a refrigerator at a temperature of -8 ℃. THF hydrate sediments were fully-formed over a period of 3-5 days.

(3) The video recorder was positioned above the sediments. The heater was turned on and the maximum output temperature was controlled by a temperature regulator. During the experiments, the environmental temperature was kept at -8 ℃. Temperature distribution and the expansion of the dissociation front were recorded by the video recorder and the temperature sensors.

(4) The hydrate-bearing sediment was heated under a constant designated temperature. When the phase transformation fronts reached the temperature sensors, the phase transformation temperature and time were recorded. The evolution of phase transformation fronts during hydrate dissociation was monitored with reference to scales in the video and temperature sensors.

Figure 3 shows the results of hydrate dissociation expansion in the sediment determined by the infrared thermometer. After the sediment was heated, the dissociation zone expanded vertically to the heat source. Two zones formed with a clearly-defined interface where the temperature was equal to the phase transformation temperature (4.4 ℃) of THF hydrate. Thus, we can infer that the hydrate dissociation zone expands as a front.

Figure 4 illustrates a comparison of the dissociation front expansion recorded by the infrared thermometer and by the temperature sensors. It can be seen that the two records are in agreement and so can be used for verifications of the theoretical model.

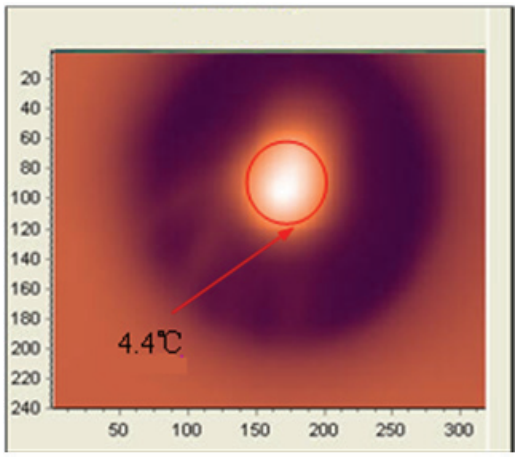

Fig.3. Observed THF hydrate dissociation front

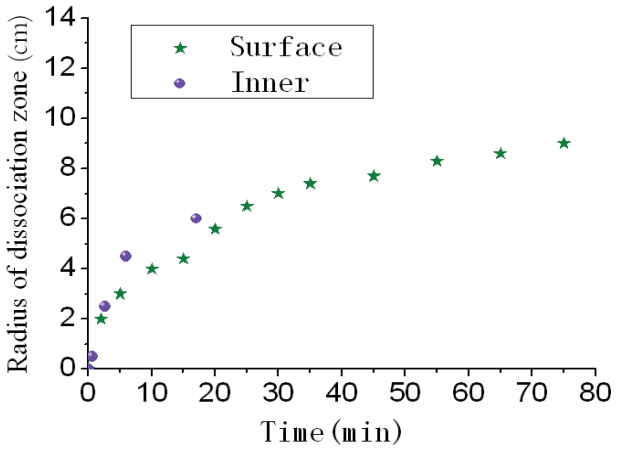

Fig. 4. Comparison of THF hydrate dissociation front at the surface and inside the sediment

ANALYSIS

Assuming the molecular formula of the hydrate is expressed as M·nH2O (M-Gas molecule, H2O- Water molecule, n-Hydrate number), the formation mechanism can be described as follows: First, the temperature of the sediment surrounding the heat source increases, causing hydrates to dissociate into water and liquid M. When the phase equilibrium temperature is reached, a hydrate dissociation zone and an un-dissociated zone are formed. These two zones are divided by a dissociation front. Second, liquid is gasified when the gasification temperature is reached, and the hydrate dissociation and gasification zones are divided by the gasification front. Finally, water is transformed into vapor when the boiling temperature is reached, and the gasification zone and the water vaporization zone are divided by the vaporization front. These three fronts expand with time.

Four cases can be observed in THF hydrate-bearing sediment: (1) If the temperature of the heat source is lower than that of hydrate dissociation, only heat conduction occurs in sediments, and the whole zone is a mixture of hydrate and the soil framework (Z1); (2) If the temperature of the heat source is greater or equal to that of hydrate dissociation and lower than that for liquid THF to gasify, there will be a phase transformation front F1, and a second zone (Z2) is formed; (3) If the temperature of the heat source is greater or equal to that for liquid THF to gasify and lower than that for water to become water vapor, there will be two phase transformation fronts F1 and F2, and a third zone (Z3) is formed; (4) If the temperature of the heat source is greater or equal to that for water to become water vapor, there will be three phase transformation fronts F1, F2 and F3, and the fourth zone Z4 is formed. The temperature distribution, phase transition front, and formation of four zones in the hydrate sediment are shown schematically in Fig. 5. As for methane hydrate-bearing sediment, case (3) will not be observed.

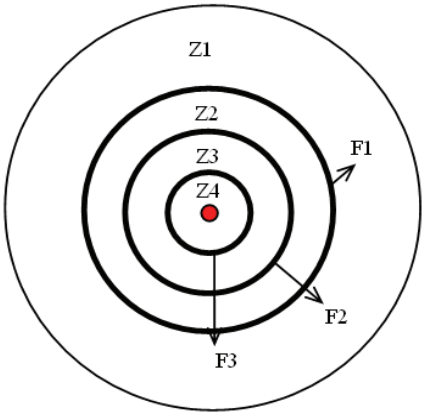

Fig.5. Zones and fronts formed during hydrate dissociation in sediments

GOVERNING EQUATIONS

In the present model is accepted and the following assumptions are made: 1) thermodynamic parameters of each phase in every miscible zone are average values. 2) enthalpies of water, liquid and hydrate are constant. Based on the mixture theory, the axi-symmetrical equation for the thermal dissociation of hydrate is obtained as follows:

Governing equation:

$$\rho C\frac{\partial T}{\partial t}=K(\frac{\partial^2 T}{\partial r^2}+\frac{1}{r}\frac{\partial T}{\partial r}) \tag{1}$$

Initial condition:

$$t=0, T=T_0 \tag{2}$$

Boundary conditions:

$$r=r_0, T=T_H \tag{3}$$

$$r=l, T=T_0 \tag{4}$$

Connecting conditions at the fronts:

$$T(s_i(t))=T_{Di} \tag{5}$$

$$K(s+)\frac{\partial T}{\partial r}\bigg|_{s_i+}-K(s-)\frac{\partial T}{\partial r}\bigg|_{s_i-}=\rho_i\Delta H_i\varepsilon_i\frac{ds_i}{dt} \tag{6}$$

The relations of volume factors:

In Z1:

$$\varepsilon_h+\varepsilon_m=1 \tag{7}$$

In Z2:

$$\varepsilon_m+\varepsilon_w+\varepsilon_f=1,\ \varepsilon_w=\frac{\rho_h\varepsilon_h M_w}{\rho_w M_h}\ \text{and}\ \varepsilon_f=\frac{\rho_h\varepsilon_h M_f}{\rho_f M_h} \tag{8}$$

In Z3:

$$\varepsilon_m+\varepsilon_w+\varepsilon_{fg}=1\ \text{and}\ \varepsilon_w=\frac{\rho_h\varepsilon_h M_w}{\rho_w M_h} \tag{9}$$

In Z4:

$$\varepsilon_m + \varepsilon_{wg} + \varepsilon_{fg} = 1 \tag{10}$$

The thermal parameters may be written as follows:

$$\rho C = \varepsilon_{fg}\rho_{fg}C_{fg} + \varepsilon_{wg}\rho_{wg}C_{wg} + \varepsilon_m\rho_m C_m \tag{11}$$

$$K = \varepsilon_{fg}K_{fg} + \varepsilon_{wg}K_{wg} + \varepsilon_m K_m \tag{12}$$

Here, i indicates the fronts of hydrate dissociation, gasification and water vaporization, respectively. f, w, h, m, wg, fg indicates liquid, water, hydrate, soil skeleton, water vapor, gas, respectively. ρ, C, K, ε, △H are density, specific heat, thermal conductivity, volume fraction, enthalpy of phase transformation, respectively. TH, T0, TDi are temperature of heat source, initial temperature of sediments, phase transformation temperature of each phase, respectively. si represents the front of phase transformation.

Substituting $\theta = T - T_0$, $\kappa = \dfrac{K}{\rho C}$ into eqs. (1)-(6), the above equations can be rewritten as follows:

Governing equation:

$$\frac{\partial\theta}{\partial t} = \frac{\kappa}{\kappa_s}\left(\frac{\partial^2\theta}{\partial r^2} + \frac{1}{r}\frac{\partial\theta}{\partial r}\right) \tag{13}$$

Initial condition:

$$t = 0, \theta = 0 \tag{14}$$

Boundary conditions:

$$r = \frac{r_0}{l}, \theta = 1 \tag{15}$$

$$r = 1, \theta = 0 \tag{16}$$

Connection conditions at fronts:

$$\theta(s_i(t)) = \frac{\theta_{Di}}{\theta_h} \quad ,$$

$$\frac{K(s+)}{K_m}\frac{\partial\theta}{\partial r}\bigg|_{s_i+} - \frac{K(s-)}{K_m}\frac{\partial\theta}{\partial r}\bigg|_{s_i-} = \frac{\kappa_m\rho_i\Delta H\varepsilon_i}{K_m\theta_h}\frac{ds_i}{dt} \tag{17}$$

NUMERICAL SIMULATIONS

A numerical method is presented here to solve eqs. (13)-(17) for analyzing the evolution of the phase transformation fronts in a finite length of HBS.

Eqs. (13)-(17) are discretized by using the Crank-Nicolson difference method.

Governing equation:

$$\frac{\theta_j^{n+1} - \theta_j^n}{\Delta t} = \frac{\kappa}{\kappa_m}\frac{1}{2(\Delta r)^2} \tag{18}$$

$$\left((\theta_{j+1}^{n+1} - 2\theta_j^{n+1} + \theta_{j-1}^{n+1}) + \theta_{j+1}^n - 2\theta_j^n + \theta_{j-1}^n) + \frac{1}{2(j+p)}(-\theta_{j+1}^n + \theta_{j-1}^n - \theta_{j+1}^{n+1} + \theta_{j-1}^{n+1})\right)$$

in which $j = 1,2,\cdots N$, $p = \dfrac{r_0}{(l - r_0)\Delta r}$.

Boundary condition:

$$\theta_0^n = 1 \tag{19}$$

$$\theta_N^n = 0 \tag{20}$$

Initial condition:

$$\theta^0 = 0 \tag{21}$$

Connecting conditions at the transformation fronts:

If the temperature at node j reaches T_{Di}/T_{Dh}, phase transformation will occur, so the temperature remains constant until the heat input equals the enthalpy for hydrate dissociation, i.e.,

$$\sum_n^{n+m}\left(\frac{\theta_{j-1}^n - \theta_j^n}{\Delta r} - \frac{\theta_j^n - \theta_{j+1}^n}{\Delta r}\right)\Delta t = \frac{\rho_i\Delta H\varepsilon_i}{\rho C\theta_{Dh}}\Delta r \tag{22}$$

The numerical simulation will proceed in the following way: after a duration of m·Δt, the phase transformation process at node j is completed, then the temperature at node j+1 will reach TDi/TDh and the phase transformation will occur at this node. Therefore, the temperature will reach T_{Di}/T_{Dh} at j+2 until the heat input equals the enthalpy for hydrate dissociation at node j+1.

The parameters are adopted as in Table 2. Specific heat of the gas was determined by the formula C=3R/M. The heat conduction coefficient is assumed to be the same as that of water vapor though in practice, it changes with temperature. Analysis shows that the approximation of the gas thermodynamic parameters has little influence on the evolution of phase transformation fronts.

RESULTS AND DISCUSSION

The thermal process are considered using a new axial symmetrical numerical method of a hydrate dissociation expansion in view of the condition of hydrate thermal recovery and oil or gas exploration under a hydrate layer. The evolution of hydrate dissociation fronts at temperatures of 50, 80, 120 and 150℃ was studied.

1) At a temperature of 50 ℃, a phase transformation front F1 formed and expanded, followed by the two zones, Z1 and Z2, formed. Expansion of the transformation front F1 was measured by temperature sensors and infrared thermometer in the experiments.

2) At a temperature of 80 ℃, phase transformation fronts F1 and F2 developed and expanded, followed by the formation of the three zones, Z1, Z2 and Z3. The expansion of the transformation front F1 was measured by temperature sensors and infrared thermometer in the experiment, but expansion of the transformation front F2 was not obtained because the color between the zone Z2 and zone Z3 could not be clearly distinguished (Z2 and Z3 shared common phases of water and sediment framework), and the temperature readings from the sensors were not obtainable because the length of Z2 and Z3 is too small.

3) At temperatures of 120 ℃ and 150 ℃, three phase transformation fronts, F1, F2 and F3, developed and expanded, followed by the formation of the four zones, Z1, Z2, Z3 and Z4. The expansion of the transformation front F3 was not apparent because it expanded too slowly.

Figure 6(a)-(d) shows that the THF hydrate dissociation front expanding velocity decreases as time increases and temperature decreases. The lengths of the THF hydrate dissociation zones are approximately linear to the square roots of time, and the experimental, analytical and numerical results are in good agreement.

Further, Thermal simulations based on our numerical method for thermal properties of methane hydrate sediments in the Shenhu area of South China Sea (Li et al., 2011) are conducted. The simulated result is that the dissociation front expands just about 15m after 20 years when the heating temperature is 298K Here we can note that the thermal simulation to the hydrate layer is neither economic nor effective, but the geological problem may be evaluate due to the slow process.

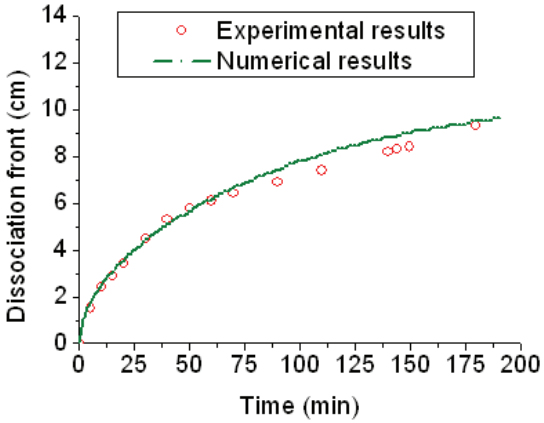

(a) Heating temperature 50℃

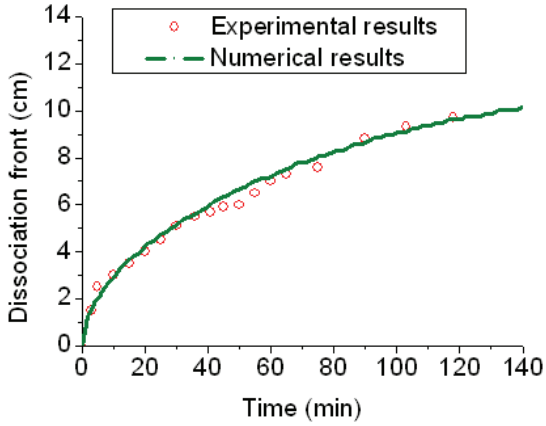

(b) Heating temperature 80℃

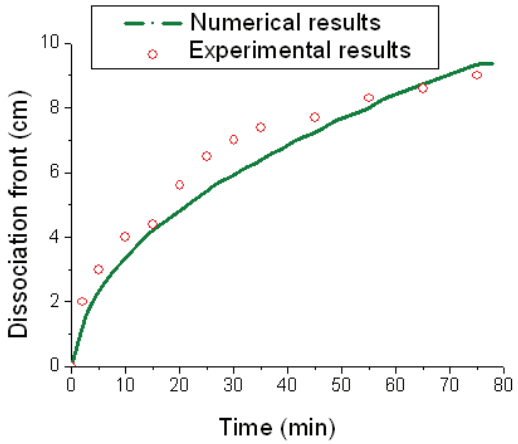

(c) Heating temperature 120℃

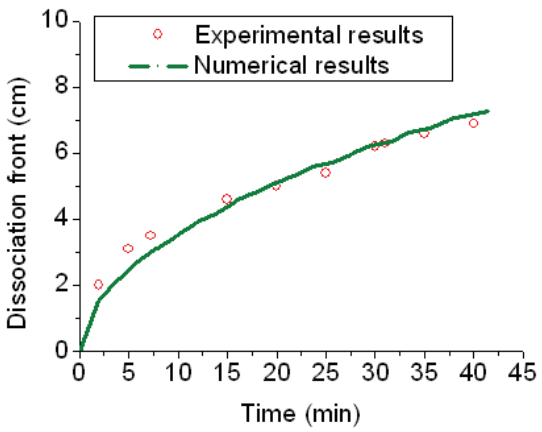

(d) Heating temperature 150℃

Fig. 6 Comparison of experimental and numerical results

CONCLUSIONS

Evolution of the hydrate dissociation zone in HBS is important for the evaluation of hazards caused by hydrate dissociation. A new axi-symmetrical model and a corresponding numerical method are proposed to analyze the thermal conduction considering one, two, three and even more phase transformation fronts. Series experiments under different temperatures were conducted by using THF hydrate-bearing sediments in an axi-symmetrical cylinder.

The results show that hydrate dissociation expands in a front style in THF hydrate-bearing sediments. The lengths of the THF hydrate dissociation zones are approximately linear to the square roots of time, and the experimental and numerical results of the expansion of the hydrate dissociation fronts are in good agreement.

This paper presents a method to evaluate the expansion of hydrate dissociation and the evolution of temperature in sediments in both hydrate exploration and deep sea exploitation of oil and/or gas when there is an overlying layer of hydrate-bearing sediment. Also it is expected that this work can be used in demonstrating the thermal processes which may lead to ground failure by hydrate dissociation.

However, only the hydrate dissociation front could be measured in the present experiments, and the development of gas seepage in sediments is ignored in the theoretical model presented here. Seepage of released gas and water and the redistribution of pore gas pressure and stresses in the sediments should be considered in the theoretical model in the future.

ACKNOWLEDGMENT

This study is part of project No.GZH201100311 funded by China Geological Survey and the National Science Foundation No.11102209

REFERENCES

Brooks, JM, Cox, BH, Bryant, WR, et al (1986). “Association of gas hydrates and oil seepage in the gulf of Mexico,” *Organic Geochemistry*, Vol 10, pp 221-234.

Briaud, JL, Chaouch, AJ (1997). “Hydrate melting in hydrate soil around hot conductor,” *J. Geotech. Geoenir. Engrg.*, Vol 123, No 7, pp 645-653.

Chaouch, A, Briaud, JL (1997). “Post melting behavior of gas hydrates in soft ocean sediments,” *OTC8298*, pp 1-11.

Hisashi, OK, Sridhar, N, Feng, S, Duane, HS (2002). “Synthesis of

methane gas hydrate in porous sediments and its dissociation by depressurizing," *Powder Tech.*, Vol 122, pp 239-246.

Jones, KW, Kerkar, PB, Mahajan, D, Lindquist, WB, Feng, H (2007). "Microstructure of natural hydrate host sediments," *Nuclear Instruments and methods in Physics Res. B*, Vol 261, pp 504-507.

Kvenvolden, KA, Lorenson, TD (2001). "The global occurrence of natural gas hydrate," *Geophysical Monograph*, Vol 124, pp 3-18.

Kwon, TH, Cho, GC, Santamarina, JC (2008). "Gas hydrate dissociation in sediments: pressure-temperature evolution," *Geochemistry Geophysics Geosystems*, Vol 9, Q03019, doi:10.1029/2007GC001920

Kimoto, S, Oka, F, Fushita, T (2010). "A chemo-thermo-mechanically coupled analysis of ground deformation induced by gas hydrate dissociation," *International Journal of Mechanical Science*, Vol 52, pp 365-376.

Klar, A, Soga, K, Ng, MYA (2010). "Coupled deformation-flow analysis for methane hydrate extraction," *Geotechnique*, Vol 60, No 10, pp 765-776.

Lee, JY, Yun, TS, Santamarina, JC (2007). "Observations related to tetrahydrofuran and methane hydrates for laboratory studies of hydrate-bearing sediments," *Geochemistry Geophysics Geosystems*, Vol 8, pp 1-10.

Li, G, Moridis, GJ, Zhang, K., Li, XS (2011). "The use of huff and puff method in a single horizontal well in gas production from marine hydrate deposits in Shenhu Area of South China Sea," *Journal of Petroleum Science and Engineering*, Vol 77, pp 49-68.

Riedel, M, Bellefleur, G, Dallimore, SR, Taylor, A, Wright, JF (2006). "Amplitude and frequency anomalies in regional 3D seismic data surrounding the Mallik 5L-38 research site, Mackenzie Delta, Northwest Territories, Canada," *Geophysics*, Vol 71, No 6, pp 183-191.

Sultan, N, Cochonat, P, Foucher, JP, Mienert, J (2004). "Effect of Gas Hydrates Melting On Seafloor Slope Instability," *Marine Geology*, Vol 213, pp 379-401.

Tohidi, B, Anderson, R, Clennell, MB, et al (2001). "Visual observation of gas hydrate formation and dissociation in synthetic porous media by means of glass micromodels," *Geology*, Vol 29, No 9, pp 867-870.

Waite, WF, Kneafsey, TJ, Winters, WJ, Mason, DH (2008). "Physical property changes in hydrate-bearing sediment due to depressurization and subsequent repressurization," *Journal of Geophysical Research*, Vol 113, B07102, doi:10.1029/2007JB005351

Xu, W, Germanovich, LN (2006). "Excess pore pressure resulting from methane hydrate dissociation in marine sediments: A theoretical approach," *Journal of Geophysical Research*, Vol 111, B011104, doi:10.1029/2004JB003600.

Yun, TS, Santamarina, JC, Rupple, C (2007). "Mechanical properties of sand, silt, and clay containing tetrahydrofuran hydrate," *Journal of Geophysical Research,* Vol 112, B04106, doi:10.1029/2006JB004484

Zhang, XH, Lu, XB, Li, QP, Yao, HY (2010). "Thermally induced evolution of phase transformations in gas hydrate sediment," *SCIENCE CHINA-Physics, Mechanics& Astronomy*, Vol 53, No 8, pp 1-6.

Zhang, XH, Lu, XB, Li, QP (2011). "Formation of layered fracture and outburst during gas hydrate dissociation," *Journal of Petroleum Engineering and Science*, Vol 76, pp 212-216.

Zhang, XH, Lu, XB, Zhang, LM, Wang, SY, Li, QP (2012). "Experimental study on mechanical properties of methane-hydrate-bearing sediments," *Acta Mechanica Sinica*, Vol 28, No 5, pp 1-11.